

PHYSIOMICS OF CORONARY PERFUSION AND CARDIAC PUMPING

FUMIHIKO KAJIYA*^{†,‡}, MASAHITO KAJIYA[‡], TARO MORIMOTO[‡],
TATSUO IWASAKI[‡], YOUSUKE INAI[‡], MASANORI HIROTA[‡],
TAKAHIKO KIYOOKA[‡], YUKI MORIZANE[‡], TAKEHIRO MIYASAKA[‡],
SATOSHI MOHRI[‡] and JUICHIRO SHIMIZU[‡]

[†]*Kawasaki Medical School*

[‡]*Okayama University Graduate School of Medicine
Dentistry and Pharmaceutical Sciences*

577 Matsushima, Kurashiki, Okayama, Japan

**kajiya@me.kawasaki-m.ac.jp*

1. Introduction

Arterial blood inflow into the myocardium is almost exclusively diastolic, whereas venous outflow is predominantly systolic.^{1,2} This finding suggests a substantial phasic volume change in the intramyocardial vessels by myocardial contraction and relaxation during a cardiac cycle. Thus, observation of the dynamics of intramyocardial microvessels during cardiac cycles is crucial for understanding the basic mechanism of intramyocardial blood perfusion. Mechanical stresses acting on intramyocardial blood vessels are different between endocardium and epicardium, hence studies of coronary hemodynamics at different transmural depths provide important information about intramyocardial influence on blood distributions in the myocardial wall. Such comparative studies may reveal why the deeper portion of myocardium is relatively vulnerable to ischemia, a principal question in coronary pathophysiology.

2. Coronary Blood Flow and Its Mechanical Interaction with Cardiac Contraction and Relaxation

Coronary vessels in the myocardium are subjected to the phasic mechanical influences of cardiac contraction and relaxation, resulting in a unique instantaneous blood flow pattern: unlike blood flow in other organs, coronary arterial flow exhibits a predominantly diastolic pattern, while venous

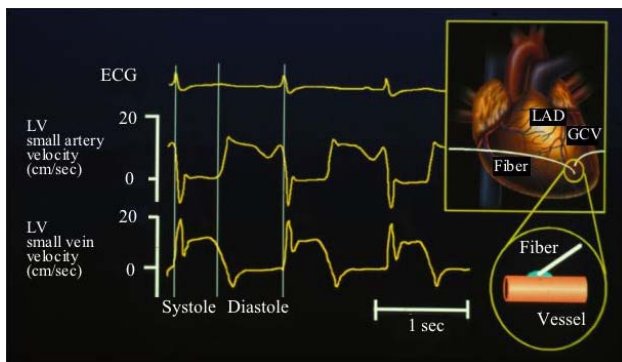


Fig. 1. Coronary arterial and venous blood velocity waveforms measured by an optical fiber sensor of laser Doppler velocimeter. The fiber sensor was fixed by cyanoacrylate adhesive on distal small artery and vein to evaluate myocardial inflow and outflow. Note the phase difference between arterial inflow and venous outflow; that is, diastolic versus systolic preponderance.

flow a systolic pattern (Fig. 1). Thus, arterial inflow into the myocardium during diastole should be stored in intramyocardial capacitance vessels (unstressed volume (UV) and ordinary capacitance), and an almost equal amount of blood should be squeezed out into epicardial veins in the next systole (Fig. 2). UV is defined as a capacitance to accommodate blood during diastole without significant increase in pressure exceeding outflow venous pressure.

To investigate the intramyocardial mechanical interaction between myocardium and coronary vessels and flow directly, we introduced a portable needle-probe video microscope with a charge-coupled device (CCD) camera to observe the subendocardial and intramural vessels.³⁻⁵ The phasic diameter of the intramural and subendocardial arterioles decreased 10–20% by cardiac contraction (Fig. 3). In contrast, the diameter of the subepicardial arterioles changes little during a cardiac cycle. Mori *et al.* observed similar systolic narrowing of perforating arterial branches with length by using synchrotron radiation angiography.⁶ The degree of systolic compression was high in deeper myocardium. More recently, using the portable needle-probe CCD video microscope with a high-speed camera (200 frame/s), the movement of visible blood flow markers (blood velocities) exhibited exclusively diastolic flow in subendocardial arterioles with two-phased systolic reverse flow, while a remarkable forward flow was recognized in subepicardial arterioles although the diastolic predominant flow pattern was common throughout myocardial layers.⁷⁻⁹

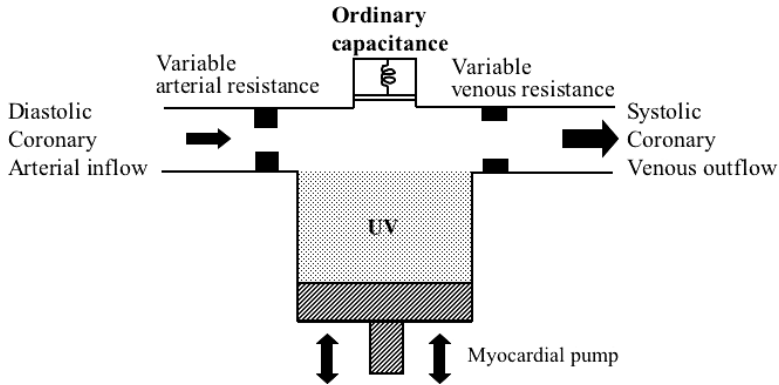


Fig. 2. Model of intramyocardial microcirculation based on Spaan *et al.*'s model. The model consists of variable arterial and venous resistances, and capacitance (UV and ordinary capacitance). UV accommodates diastolic arterial inflow without increase of UV pressure above outflow venous pressure. During systole, myocardial pump (pressure) propels pooled blood in UV to coronary vein.

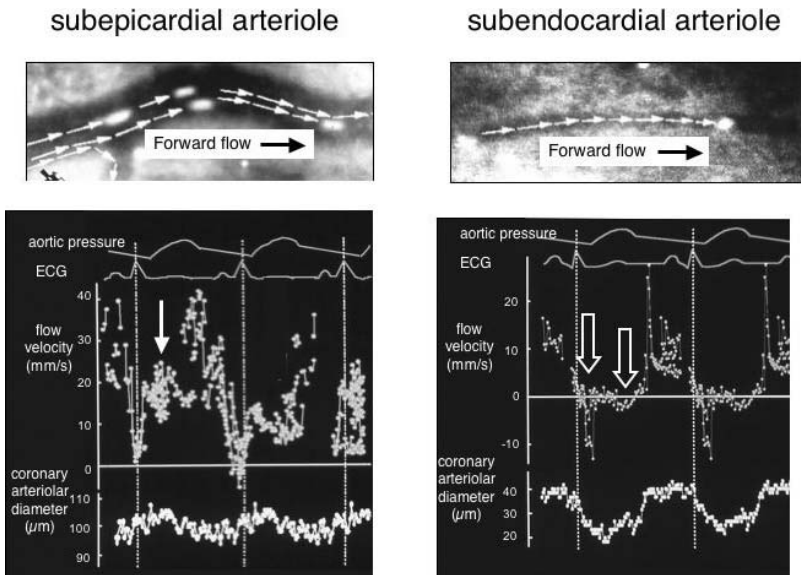


Fig. 3. Subepicardial and subendocardial arteriolar images with flow markers. Although diastolic predominant pattern is similar between subepicardium and subendocardium, remarkable systolic forward flow (\downarrow) is observed in subepicardial arterioles, while negligibly small forward flow with two-phased reverse flows (\uparrow) is noticed in subendocardium. The diameter of subendocardial arterioles decreased in systole by 10–20%, while that of subepicardium almost remained unchanged (revised from Ref. 9).

3. Functional Role of Capillaries As Capacitance and UV Through Myocardial Wall

To clarify the functional characteristics of intramyocardial capillaries, as well as possible transmural difference, we visualized the 3D capillary architecture by intracoronary injection of custom-made contrast medium consisting of BaSO₄, India ink, gelatin, and distilled water in diastolic- and systolic-arrest rat hearts.¹⁰ A confocal laser-scanning microscope (CLSM) was used for the 3D microvisualization, and 200- μm -thick block sample was used after slicing by a microtome.

Figure 4 shows epimyocardial (left) and endomyocardial (right) capillary images during diastole (top) and systole (bottom). Capillary volume decreased by 32% on average throughout myocardium. The volume fraction of capillaries per unit myocardial mass is 10 times as large as that of arterioles and venules, indicating that capillaries function as major capacitance and UV (see Fig. 2).

Transmurally, the reduction in volume fraction of capillary from systole to diastole was by 37% in endocardium, by 34% in midcardium, and by 19% in epicardium (Fig. 5). Thus, the functions of capillaries as capacitance may be more remarkable in the deeper layers.

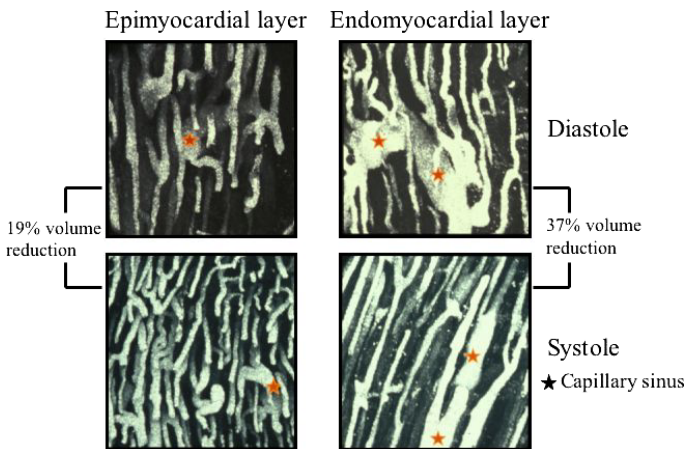


Fig. 4. Epimyocardial (left) and endomyocardial (right) capillary images in diastolic (top) and systolic arrested rat hearts. Note that the capillary diameters decreased in both epi- and endomyocardial layers during systole, but the degree is greater in endomyocardium. The capillary sinus is also compressed during systole, especially in endomyocardial layer.

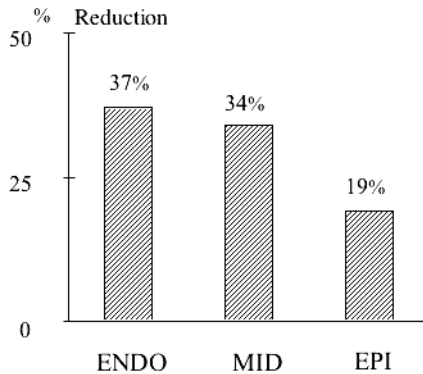


Fig. 5. Volume reduction of transmural capillaries from diastole to systole. Volume reduction by cardiac contraction is most remarkable in endomyocardium (ENDO), while that of epimyocardium (EPI) is half of endomyocardium. The midmyocardial (MID) volume change is little less than endomyocardium (revised from Ref. 10).

4. Capillary Flow Dynamics and Regional Myocardial Perfusion

Recently, we visualized the epicardial capillary network of the beatings in dog hearts *in vivo*, using high-resolution needle-lens probe microscope (Fig. 6).¹¹ A capillary originating from a point in an arteriolar zone carries blood running parallel to the muscle fibers and ends in a point in the venular zone. The capillary length from the smallest arteriole and venule is several hundred μm .⁷ This path length is 8–10 times larger than a single capillary length, indicating 8–10 interconnection along the path length. The flow through Y-, T-, H-, and hairpin-type interconnection seen in the CLSM image (Fig. 4) was recognized by *in vivo* visualization. The flow of neighboring capillaries exhibited co- and counter-currents, and cross-connecting flow occurred abundantly through interconnection, facilitating oxygen supply to myocytes.

The transit time of blood in the capillary path length was about 1.5 s, again indicating that the capillary works as UV, which stores the arterial inflow blood for this period without emergence of venous flow.¹² The other characteristics of capillary hemodynamics were coexistence of systolic and diastolic preponderant flows. This coexistence of temporal flow preponderance implies that the watershed between diastolic arterial and systolic venous flows is located within capillaries. The diastolic preponderance may be arteriolar capillary, while the systolic is venular one.

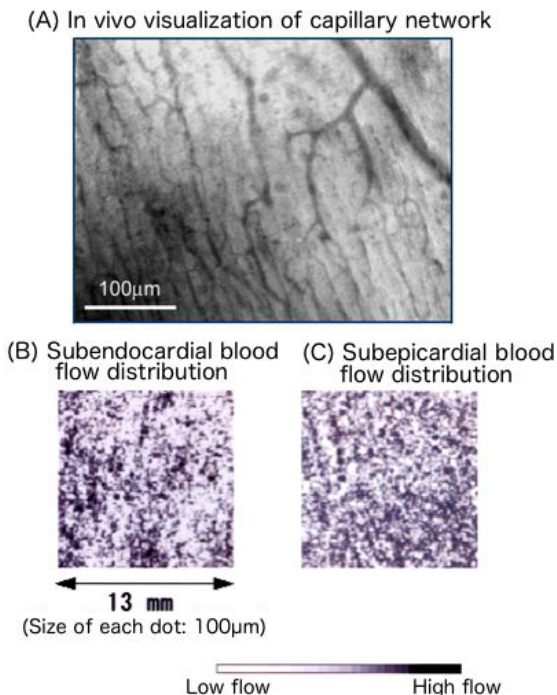


Fig. 6. Visualization of coronary capillary network in dogs with our high-magnification needle-lens CCD microscope (A). Microblood flow distribution by tracer autoradiography with ^3H -desmethyl-imipramine in rabbit subendocardial and subepicardial layers (B, C). Note the dense capillary network with H-, Y-, T-, and hairpin-type interconnection. There is coexistence of systolic and diastolic preponderant flow through capillary network (A). Marked global microheterogeneity (high flow in one region, but low flow in other region) of blood flow is recognized in subendocardial layer, while local (point-to-point) heterogeneity is more remarkable in subepicardial layer (revised from Refs. 12–14).

In Fig. 6, flow distributions within subendocardial (B) and subepicardial (C) layers of a rabbit left ventricular wall are shown. These images were obtained by tracer digital radiography with $100\text{-}\mu\text{m}$ resolution.^{13,14} Both show a marked spatial heterogeneity as quantitated by the coefficient of variation of flows ($\text{CV} = \text{standard deviation}/\text{mean}$) and the correlation coefficient of adjacent regional flows (CA). Both CA and CV values are higher in subendocardium than in subepicardium, indicating the existence of more clearly distinct aggregates of high or low regional flows in subendocardium. The greater anatomic myocardial flow heterogeneity may explain the greater CV in subendocardium, which is inferred from the higher flow

heterogeneity in subendocardium observed in the fully vasodilated, arrested heart.¹⁵ In addition, the extravascular compressible force may also contribute to the transmural difference of CV and CA, because its enormous effect on subendocardium^{3,5} appears to vary spatially to the larger extent within subendocardium than subepicardium due to the existence of the papillary muscle.

5. Simulation of Intramyocardial Microcirculation

We modified the intramyocardial pump model originally proposed by Spaan *et al.*¹⁶ In our model, the myocardium was divided into three layers.¹⁷ The vascular compartments of each layer were consisted of arterioles, capillaries, and venules. A lumped epicardial artery was placed proximal to all of these layers, and a lumped vein was placed distally (Fig. 7).

Intramyocardial vascular diameter is determined by a transmural pressure ($P_{TR} = P - P_{im}$) and a vascular elasticity, wherein P is intravascular pressure and P_{im} intramyocardial pressure. To calculate instantaneous blood volume in each compartment, P_{im} was assumed to be 5/6 of left ventricular pressure (LVP) at subendocardial layer, 3/6 at midmyocardial layer, and 1/6 at subepicardial layer assuming endo-, mid-, and epimyocardial compartments located at the depth of 1/6, 3/6, and 5/6 from endocardium, respectively, because it is well documented that the intramyocardial hydrostatic pressure decreased almost linearly from endocardium to epicardium. The relation between vascular volume (V) in each compartment and transmural pressure (P_{TR}) can be expressed by

$$P_{TR} = A \exp(Ke(t)V) + B \log(Ke(t)V) - P_0. \quad (1)$$

Here, the elastance of a vessel consists of two components: (i) The first component is the time-dependent elastance relating to local myocardial stiffness. This implies that vascular elastance increases with increasing cardiac stiffness during systole (by crossbridge formation) and decreases with decreasing of stiffness during diastole. This is expressed by the time-dependent parameter $Ke(t)$, which is based on Krams *et al.*'s article,¹⁸ extended from Suga's original work.¹⁹ Since cardiac contractility is considered to be uniform transmurally, $Ke(t)$ value is set to be equal in all three layers. (ii) The second component involves vascular stiffness changes following the state of contraction and relaxation of vascular smooth muscle itself. This is modeled by change in the time-independent parameter A , B ,

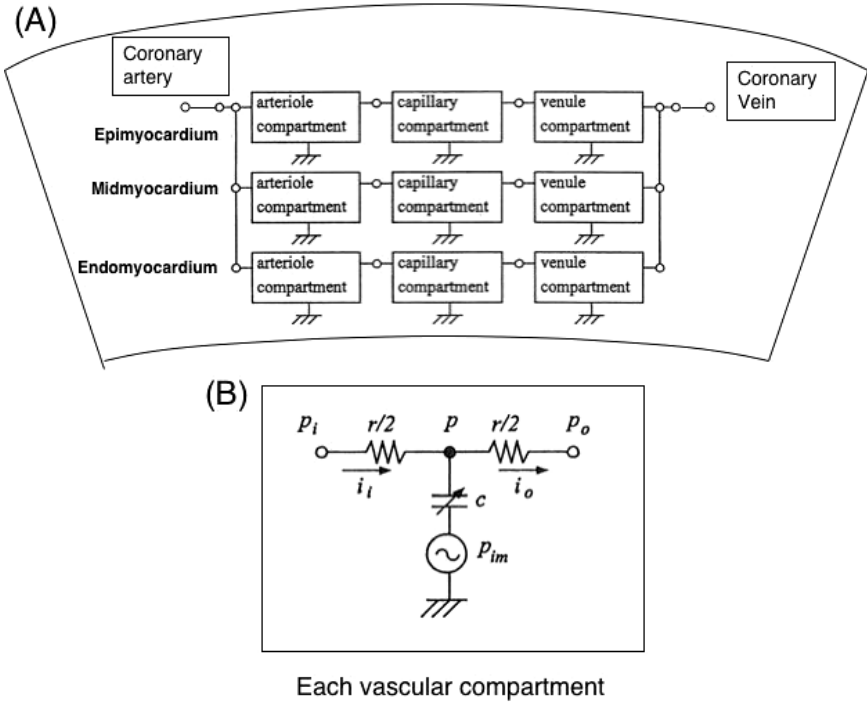


Fig. 7. Three layers (epi-, mid-, and endomyocardium) coronary circulation model consisting of nine vascular compartments based on Spaan *et al.*'s model. Each compartment is basically same, but intravascular and intramyocardial pressures, and vascular compliance C of each compartment are different transmurally and temporally. C relates to parameters k, a, b and P_0 in Eq. (1). The resistance (r) was calculated from the volume V stored in C by the Poisuille law, and is located in proximal and distal portions of each compartment on a fifty-fifty basis.

and P_0 in Eq. (1). The values of these constants of each vascular compartment are determined based on published data^{17,20} and our own animal experimental data. Resistance is represented to be inversely proportional to square of vascular volume,¹⁶

$$R = K_r/V^2, \tag{2}$$

where K_r is a constant, the value of which is also given as in our earlier report.²¹ We input a typical measured data of aortic pressure and LVP obtained from our laboratory.

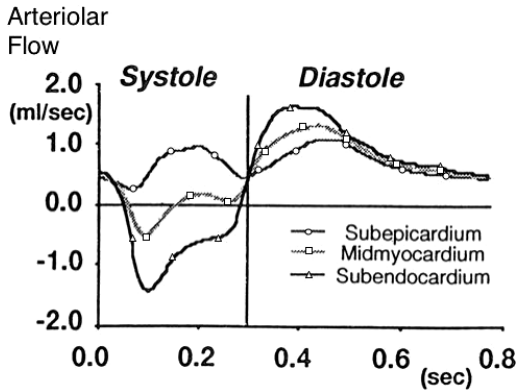


Fig. 8. Simulated blood flow waveforms in subepicardial, midmyocardial, and subendocardial arterioles. Note that there is systolic reverse flow in deeper myocardium, while systolic forward flow in superficial portion. The amount of diastolic flow component is larger in deeper portion.

Figure 8 shows an example of our simulation results of arteriolar flows simulation in three different layers.¹⁷ In subendocardium, two-peaked systolic retrograde flow with predominant diastolic flow was simulated, as seen in our *in vivo* visualization experiments (see Fig. 3). The subepicardial arteriolar flow exhibited two peaked forward flows, one during systole and the other during diastole, consistent with our experimental data except a sharp and short dip during isovolumic contraction phase, probably due to local muscle strain. The flow pattern in the arteriole in midlayer exhibited an in-between pattern, but we have no available experimental data at present.

The diameters of subendocardial and midmyocardial arterioles decreased during systole as our physiologic measurements, and the degree of diameter change was greater in the deeper myocardium (data not shown). The subepicardial arterioles changed very little, which is also good agreement with our experiments.

Figure 9 shows a simulation study result of transmural autoregulation of coronary circulation. When the coronary perfusion pressure decreased from normal physiologic pressure to about 70 mmHg, coronary flow in all layers did not change; that is, autoregulatory mechanism operated well. However, when the coronary perfusion pressure further decreased, the subendocardial flow began to decrease, while autoregulation still operated in mid- and subepicardial layers. Further pressure decrease less than 60 mmHg caused

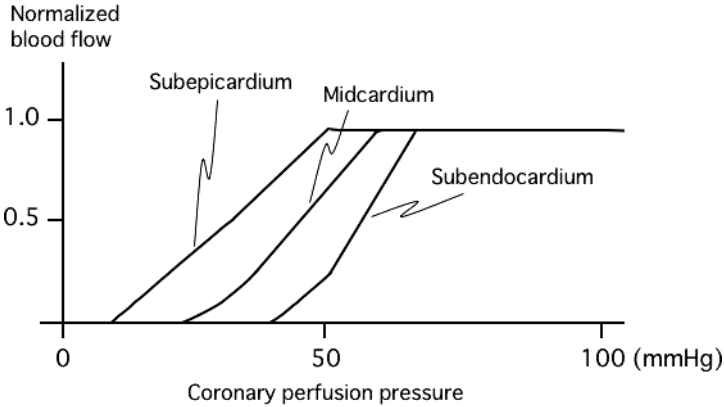


Fig. 9. Computer simulation of autoregulation of subepicardial, midcardial, and subendocardial microvessels. Note that autoregulation is working more robustly in subepicardial layer than subendocardial layer. The autoregulation in midcardium lies in-between.

disappearance of autoregulation of midlayer, and finally subepicardial regulation waned for lower pressure range below 50 mmHg. Collectively, this simulation study confirmed that epimyocardial layers are robust against ischemia, while endomyocardial layers are weakest and midcardial layers in-between.

6. Capillary As Capacitance and Its Effect on Coronary Arterial Inflow and Venous Outflow

Figure 10 shows the relation between coronary arterial inflow and blood-pooled conditions in UV.²² The protocol of this experiment in an AV-blocked dog was as follows: the blood pooled in capacitance vessels (mainly UV) was squeezed out until coronary venous flow became nearly zero by cardiac contractions after coronary artery (left anterior descending artery, LAD) occlusion and then long diastole was induced by pacing-off. During long diastole, LAD perfusion pressure was increased stepwise (two levels). After application of LAD perfusion pressure, the great cardiac vein (GCV) flow was absent for 1 or 2 s, indicating that UV was not filled yet. Then, the GCV flow resumed and gradually increased, indicating filling of UV. It is noticeable that the LAD flow was significantly higher in UV-unfilled conditions than in UV-filled conditions. This is physiologically important as a biomechanical feedback mechanism that pooled blood volume in the capacitance vessels exceeding UV reduces coronary arterial inflow.

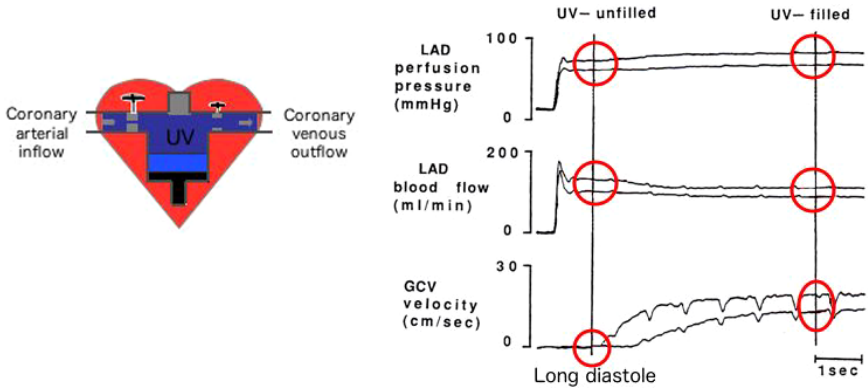


Fig. 10. Coronary arterial (LAD) flow and GCV flow responses to stepwise increase in LAD perfusion pressure during artificially induced long diastole. After perfusion pressure increase, GCV flow was absent for 1 or 2 s, indicating that UV is unfilled, and then GCV flow increased gradually; that is, UV filled. Note that LAD flow in UV unfilled is greater than that in filled condition. This implies that the blood volume pooled in UV has a mechanical feedback control against coronary arterial inflow (revised from Ref. 22).

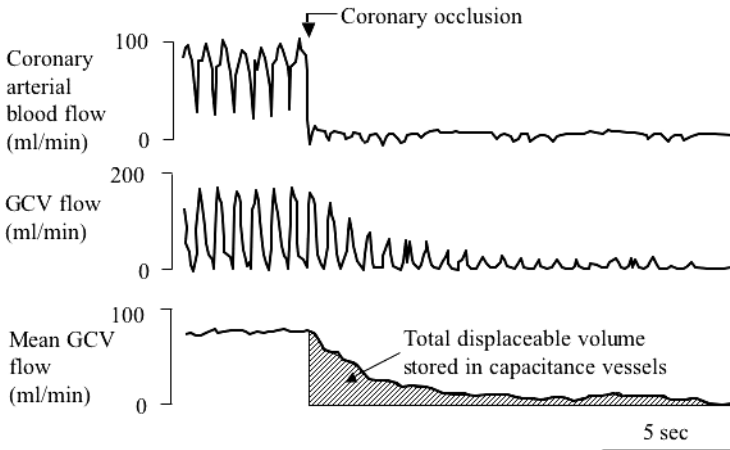


Fig. 11. A typical example of the decaying process of the coronary venous flow velocity after coronary inflow occlusion. The GCV flow decreased exponentially.

Figure 11 shows arterial and venous flows before coronary inflow occlusion and the decay phenomenon process of the GCV flow velocity after occlusion. It should be noted that the adjusted mean GCV flow averaged for each beat decreased exponentially.²³ Thus, the process can be

expressed as

$$V_{GCV}(t) = V_{GCV}(0) e^{-t/\tau}, \tag{3}$$

where $V_{GCV}(t)$ is the decaying flow after the coronary artery occlusion, $V_{GCV}(0)$ is the mean flow just before occlusion, and τ is the decaying time constant. Integration of Eq. (3) with respect to time t gives

$$\int_0^\infty V_{GCV}(0)e^{-t/\tau} dt = V_{GCV}(0) \tau. \tag{4}$$

The value of $V_{GCV}(0)\tau$ represents the total displaceable volume V_0 (mainly UV) stored in the intramyocardial capacitance vessels before occlusion:

$$V_0 = \tau V_{GCV}(0). \tag{5}$$

Alternatively,

$$V_{GCV}(0) = V_0/\tau. \tag{6}$$

Figure 12 depicts this relationship between coronary venous outflow $V_{GCV}(0)$ and the total displaceable volume V_0 . The correlation coefficient between the total displaceable volume V_0 and the coronary vein flow $V_{GCV}(0)$ at one beat before occlusion was significantly high ($r = 0.86$, $p < 0.01$), whereas the time constant is almost constant irrespective of various coronary venous flows ($\tau \approx 1.8$ s). This result implies that the greater

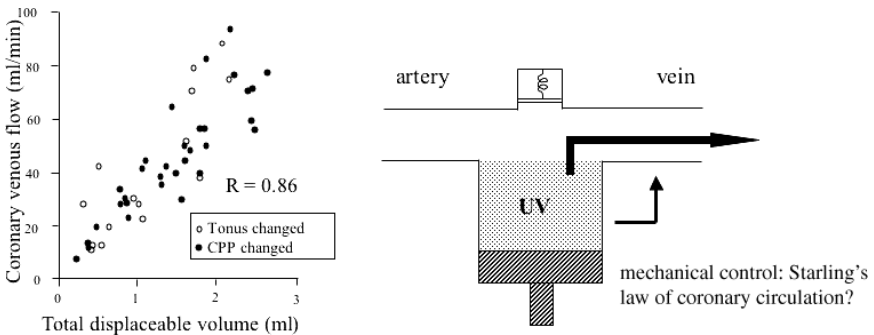


Fig. 12. Relationship between venous outflow and total displaceable blood volume in intramyocardial capacitance vessels (left) and positive feedback from total displaceable blood volume to venous outflow (right). Coronary perfusion pressure (CPP) or coronary vascular tonus were changed to obtain the scatter diagram (left). In spite of wide variation of CPP and vascular tone, the correlation coefficient is significantly high. The observation that increase in total displaceable volume in UV augments venous outflow indicates the mechanical feedback from stored blood in UV to venous flow (right).

the blood volume stored in the capacitance vessels, the more the venous blood flow out (Fig. 12 (left)). This can draw an analogy to the Starling's law of the heart, namely: more the blood stored in the left ventricle during diastole, more the blood pumped out into aorta in the next systole (Fig. 12 (right)). In other words, there is a positive feedback from the stored blood volume in capacitance vessels to venous outflow. We also found that there is a negative feedback from the stored blood in diastole to diastolic arterial inflow; that is, the more the blood stored in diastole, the less the blood inflow in the same diastole.

7. Conclusion

In conclusion, a physiomic understanding of mechanical interaction between coronary microcirculation and cardiac pumping is fundamentally important to the understanding of intramural coronary hemodynamics. The transmural morphology and function of capillaries are the key issues for the mechanical control of coronary circulation together with arteriolar and venular mechanics.

Acknowledgments

The authors thank Drs. M. Goto, T. Yada, E. Toyota, T. Matsumoto, O. Hiramatsu, Y. Ogasawara, K. Tsujioka and T. Okamoto for their collaboration of studies. Thanks are also given to Ms. H. Izushi, E. Nawachi and K. Yoshioka for their help in the preparation of this manuscript.

This study was partly supported by Grants-in-Aid for Scientific Research from the Ministry of Education, Science, Technology, Sports and Culture (S and A), and the Research Grant for Cardiovascular Diseases (14-1) from the Ministry of Health, Labor and Welfare. We are grateful to World Scientific, for permission to reproduce in part our paper published in JMMB Vol. 5 No. 1 (2005) 1–9²⁴.

References

1. W. M. Chilian, and M. L. Marcus, Phasic coronary flow velocity in intramural and epicardial coronary arteries, *Circulation Research* **50**, 6 (1982) 775–781.
2. F. Kajiya, G. Tomonaga, K. Tsujioka, Y. Ogasawara, and H. Nishihara, Evaluation of local blood flow velocity in proximal and distal coronary arteries by laser Doppler Method, *Journal of Biomechanical Engineering* **107**, 1 (1985) 10–15.

3. T. Yada, O. Hiramatsu, A. Kimura, M. Goto, Y. Ogasawara, K. Tsujioka, S. Yamamori, K. Ohno, H. Hosaka, and F. Kajiya, In vivo observation of subendocardial microvessels of the beating porcine heart using a needle-probe videomicroscope with a CCD camera, *Circulation Research* **72**, 5 (1993) 939–946.
4. F. Kajiya, T. Yada, A. Kimura, O. Hiramatsu, M. Goto, Y. Ogasawara, and K. Tsujioka, Endocardial coronary microcirculation of the beating heart, *Advances in Experimental Medicine and Biology* **346** (1993) 173–180.
5. O. Hiramatsu, M. Goto, T. Yada, A. Kimura, Y. Chiba, H. Tachibana, Y. Ogasawara, K. Tsujioka, and F. Kajiya, In vivo observations of the intramural arterioles and venules in beating canine hearts, *Journal of Physiology* **509**, 2 (1998) 619–628.
6. H. Mori, E. Tanaka, K. Hyodo, M. Uddin Mohammed, T. Sekka, K. Ito, Y. Shinozaki, A. Tanaka, H. Nakazawa, S. Abe, S. Handa, M. Kubota, K. Tanioka, K. Umetani, and M. Ando, Synchrotron microangiography reveals configurational changes and to-and-for flow in intramyocardial vessels, *American Journal of Physiology* **276**, 2 (1999) H429–H437.
7. F. Kajiya, and M. Goto, Integrative physiology of coronary microcirculation, *Japanese Journal of Physiology* **49**, 3 (Review) (1999) 229–241.
8. F. Kajiya, T. Yada, T. Matsumoto, M. Goto, and Y. Ogasawara, Intramyocardial influences on blood flow distributions in the myocardial wall, *Ann Biomed Eng* **28**, 8 (Review) (2000) 897–902.
9. E. Toyota, Y. Ogasawara, O. Hiramatsu, H. Tachibana, F. Kajiya, S. Yamamori, and W. M. Chilian, The dynamics of flow velocities in endocardial and epicardial coronary arterioles, *American Journal of Physiology* **288**, 4 (2005) H1598–1603.
10. E. Toyota, K. Fujimoto, Y. Ogasawara, T. Kajita, F. Shigeto, T. Matsumoto, M. Goto, and F. Kajiya, Dynamic changes in three-dimensional architecture and vascular volume of transmural coronary microvasculature between diastolic- and systolic-arrested rat hearts, *Circulation* **105**, 5 (2002) 621–626.
11. T. Kiyooka, O. Hiramatsu, F. Shigeto, T. Yamamoto, H. Nakamoto, T. Yada, Y. Ogasawara, T. Morimoto, Y. Morizane, H. Minami, S. Mohri, J. Shimizu, T. Ohe, and F. Kajiya, Functional role of capillaries in reactive hyperemia by direct observation with a pencil-lens intravital videomicroscope, *Microcirculation Annual 2003*, eds. M. Asano and S. Miura (Nihon-Igakukan, Tokyo, 2003) 63–64.
12. T. Kiyooka, O. Hiramatsu, F. Shigeto, H. Nakamoto, H. Tachibana, T. Yada, Y. Ogasawara, M. Kajiya, T. Morimoto, Y. Morizane, S. Mohri, J. Shimizu, T. Ohe, and F. Kajiya, Direct observation of epicardial coronary capillary hemodynamics during reactive hyperemia and during adenosine administration by intravital videomicroscopy, *American Journal of Physiology* **288**, 3 (2005) H1437–1443.
13. T. Matsumoto, M. Goto, H. Tachibana, Y. Ogasawara, K. Tsujioka, and F. Kajiya, Microheterogeneity of myocardial blood flow in rabbit hearts during normoxic and hypoxic states, *American Journal of Physiology* **270** (1996) H435–441.

14. T. Matsumoto, J. Ebata, H. Tachibana, M. Goto, and F. Kajiya, Transmural microcirculatory blood flow distribution in right and left ventricular free walls of rabbits, *American Journal of Physiology* **277** (1999) H183–191.
15. R. E. Austin, Jr, N. G. Smedira, T. M. Squiers, and J. I. Hoffman, Influence of cardiac contraction and coronary vasomotor tone on regional myocardial blood flow, *American Journal of Physiology* **266**, 6 Pt 2 (1994) H2542–2553.
16. P. Bruinsma, T. Arts, J. Dankelman, and J. A. Spaan, Model of coronary circulation based on pressure dependence of coronary resistance and compliance, *Basic Research in Cardiology* **83**, 5 (1988) 510–524.
17. S. Ohta, Y. Ogasawara, T. Matsumoto, O. Hiramatsu, H. Nakamoto, T. Okamoto, and F. Kajiya, Analysis of coronary haemodynamics by coronary circulation model with three layered myocardium, *IEEE Computers in Cardiology* (1995) 673–677.
18. R. Krams, P. Sipkema, and N. Westerhof, Varying elastance concept may explain coronary systolic flow impediment, *American Journal of Physiology* **257**, 26 (1989) H1471–1479.
19. H. Suga, K. Sagawa, and A. A. Shoukos, Load independence of the instantaneous pressure-volume ratio of the canine left ventricle and effects of epinephrine and heart rate on the ratio, *Circulation Research* **32**, 3 (1973) 314–322.
20. J. Dankelman, H. G. Stassen, and J. A. Spaan, Coronary circulation mechanics, *Coronary Circulation-Basic Mechanism and Clinical Relevance* eds. Kajiya *et al.* (Springer-Verlag, Tokyo, 1990), 75–87.
21. F. Kajiya, T. Yada, T. Matsumoto, M. Goto, and Y. Ogasawara, Intramyocardial Influences on blood flow distributions in the myocardial wall, *Annals of Biomedical Engineering* **28**, 8 (2000) 897–902.
22. M. Goto, K. Tsujioka, Y. Ogasawara, Y. Wada, S. Tadaoka, O. Hiramatsu, M. Yanaka, and F. Kajiya, Effect of blood filling in intramyocardial vessels on coronary arterial inflow, *American Journal of Physiology* **258** (1990) H1042–1048.
23. F. Kajiya, O. Hiramatsu, M. Goto, and Y. Ogasawara, Mechanical characteristics of coronary circulation, *Journal of Mechanics in Medicine and Biology* **1**, 2 (2001) 67–77.
24. M. Kajiya, O. Hiramatsu, T. Yada, E. Toyota, T. Kiyooka, S. Mohri, J. Shimizu, Y. Ogasawara, and F. Kajiya, Physiomic approach to biomechanics of coronary microcirculation, *Journal of Mechanics in Medicine and Biology* **5**, 1 (2005) 1–9.